The structures and electronic properties of Lan and LanO (n=2–12) clusters

ARTICLE *in* CHEMICAL PHYSICS · MAY 2009

Impact Factor: 1.65 · DOI: 10.1016/j.chemphys.2009.03.010

5 AUTHORS, INCLUDING:

Yi-Xiang Wang
Jiangnan University
18 PUBLICATIONS **47** CITATIONS
SEE PROFILE

Ai-Min Guo
Chinese Academy of Sciences
23 PUBLICATIONS **181** CITATIONS
SEE PROFILE

Shi-Jie Xiong
Nanjing University
275 PUBLICATIONS **1,732** CITATIONS
SEE PROFILE

Chemical Physics 359 (2009) 82–91

Contents lists available at ScienceDirect

Chemical Physics

journal homepage: www.elsevier.com/locate/chemphys

The structures and electronic properties of La_n and La_nO (n = 2–12) clusters

Z. Yang *, Y.X. Wang, A.M. Guo, H.J. Zhu, S.J. Xiong

National Laboratory of Solid State Microstructures and Department of Physics, Nanjing University, Nanjing 210093, China

ARTICLE INFO

Article history:
Received 25 January 2009
Accepted 13 March 2009
Available online 21 March 2009

Keywords:
DFT
Cluster

ABSTRACT

The density functional theory (DFT) has been used to determine the binding energies, ground state structures, electronic properties, and magnetic properties of La_n and La_nO (n = 2–12) clusters. For La_n, the lowest-energy structures of La_4, La_8, and La_9 clusters are the new ones that have not been proposed in previous literature. These structures are more stable and are confirmed by CCSD(T) method. For La_nO, we find that the O atom prefers to stay at the outside of the cluster, and the coordination number gradually increases with cluster size. Furthermore, the results for average magnetic moments of La_n clusters are in good agreement with experiment, implying that present treatments are reasonable and reliable. In addition, our results show that the ionic and covalent bonding characteristics are important in small La clusters.

1. Introduction

During the last few years, the structural and electronic properties of transition metal (TM) clusters have been extensively studied because of their fundamental properties and potential applications in nanotechnology [1–3]. One typical example is the lanthanum cluster. In earlier time the Möbius inversion pair potential in combination with genetic algorithm (GA) was used to explore the lowest-energy structures of the La_{3-20} clusters, and the energetics and structural stability of La clusters with number of atoms n = 3–13 were investigated by performing molecular dynamics (MD) simulations with an empirical potential [4,5]. Then, more accurate density functional theory (DFT) was employed to study the structural stability and electronic structure of La_n, and to predict the magnetic properties of the clusters [6,7]. Recently, Knickelbein has measured the magnetic moments in clusters of the group-III transition elements (Sc_n, Y_n, and La_n (n = 5–20)) in the Stern–Gerlach molecular beam deflection experiment [8]. The experimental results suggest that the La_6 has particularly strong enhancement of magnetism, 4.8 ± 0.2 μ_B, while other small lanthanum clusters are in the lower spin states, and that the pure Sc_n and Y_n clusters exhibit very similar size dependence of magnetism. In parallel with this experiment, another DFT study about pure La_n (n = 2–14) clusters was carried out and discussed [9]. However, some conclusions in these two DFT studies (Refs. [6,9]) are inconsistent. For example, the lowest-energy structures of La_{8-14} clusters proposed in these two papers are different. More importantly, some electronic properties of pure La_n clusters, such as ionization potential and electron affinity, are still unknown so far. Therefore, the stable structures and the electronic properties of pure La_n clusters need to be further verified and investigated.

Besides the pure lanthanum clusters, the doped lanthanum clusters have become another fascinating subject of widespread investigations in recent years. The structures and magnetic moments of small lanthanum–nickel clusters have been systematically calculated with DFT [10]. The M-doped La_{13} clusters (M = B, Al, Ti, Ni, C, and Si) have been recently reported [11,12]. In addition, transition metal oxide cations of the form $M_nO_m^+$ (M = Y and La) are produced by laser vaporization in pulsed nozzle source and detected with time-of-flight mass spectrometry [13]. These doped lanthanum clusters exhibit very interesting and novel chemical and physical properties, which are quite different from the pure lanthanum clusters.

It is well accepted that doped atom can dramatically modify many properties of pure clusters in a variety of ways. Taking pure Sc_n and Y_n clusters as an example, as mentioned above, the experimental results show that the Sc_n and Y_n clusters have a very similar size dependence of magnetism. Theoretical studies well reproduce the experimental data and therefore confirm the similarity [14,15]. In two recent papers, we systematically investigated the O-doped scandium clusters and O-doped yttrium clusters (Sc_nO and Y_nO) [16,17]. Interestingly, we find that the O atom can greatly enhance the total magnetic moments of the Sc_n clusters. The total magnetic moments of Sc_nO are larger than those of Sc_n clusters at n = 4 and 7–12. However, for Y_nO, we do not find significantly enhanced moments as compared with pure Y_n clusters. In other words, the magnetism of Sc_nO is different from that of Y_nO, and the similarity of the magnetism of the pure clusters is destroyed after doping O atom. Then, what will happen when adding one O atom to lanthanum clusters? How does the O atom influence the magnetism of lanthanum clusters? These should be

* Corresponding author.
E-mail address: yzcluster@sina.com (Z. Yang).

0301-0104/$ - see front matter © 2009 Elsevier B.V. All rights reserved.
doi:10.1016/j.chemphys.2009.03.010

very interesting questions and therefore, could become another focus of further research.

With this in mind, in this paper we present a detailed investigation on geometric, electronic, and magnetic properties of La_n and La_nO clusters (n = 2–12) by using DFT method. We discuss the geometrical and electronic properties of the two systems, such as the stable structures, relative stability, energy gaps between highest occupied molecular orbital (HOMO) and lowest unoccupied molecular orbital (LUMO), and total and local magnetic moments. The paper is arranged as follows: In Section 2, we discuss computational methods briefly. Our results and discussion are presented in Section 3. Finally, the conclusion is drawn in Section 4.

2. Computational methods

The structural optimizations are performed using the DFT with general gradient approximation (GGA) corrected-exchange potential constructed by combing the Perdew and Wang correlation functional with Beck's exchange functional (BPW) as implemented in DMOL package [18]. For heavy elements such as lanthanum, the relativistic effects are important. Thus we performed all-electron spin-unrestricted calculations with relativity, and a basis set composed of double numerical basis (5d and 6s) with polarized function (6p) (DNP) is used. For accurate evaluation of the charge density, we chose the octuple scheme for the multipolar fitting procedure and a fine grid scheme for the numerical integration. In addition, the direct inversion in an iterative subspace (DIIS) approach is used to speed up the SCF convergence. The convergence criteria of optimization are 0.001 eV/Å and 0.001 Å for energy gradient and atomic displacement, respectively. The charge density is convergent to 1×10^{-6}, which corresponds to a total energy convergence of 1×10^{-5} eV.

We first optimized the structures of La_n clusters. For small clusters with less than five La atoms, all possible structures are considered, including linear chains, planer structures, and three-dimensional (3D) structures. As the cluster size increases, the number of possible geometries increases dramatically. The energy surface of even a 6-atom lanthanum cluster is complicated and the unbiased searches of the configuration and spin multiplicities at first-principles level are computationally very demanding. So, as initial geometries we started with the structures of analogous sizes that have been discussed previously [14–16]. Moreover, a lot of initial structures of larger clusters are designed by hand. For instance, we can often simply add or subtract an atom from a cluster of size n to obtain geometry for a cluster of size $n + 1$ or $n - 1$, or construct the initial structures according to a certain symmetry. Furthermore, the stable structures for the pure lanthanum clusters

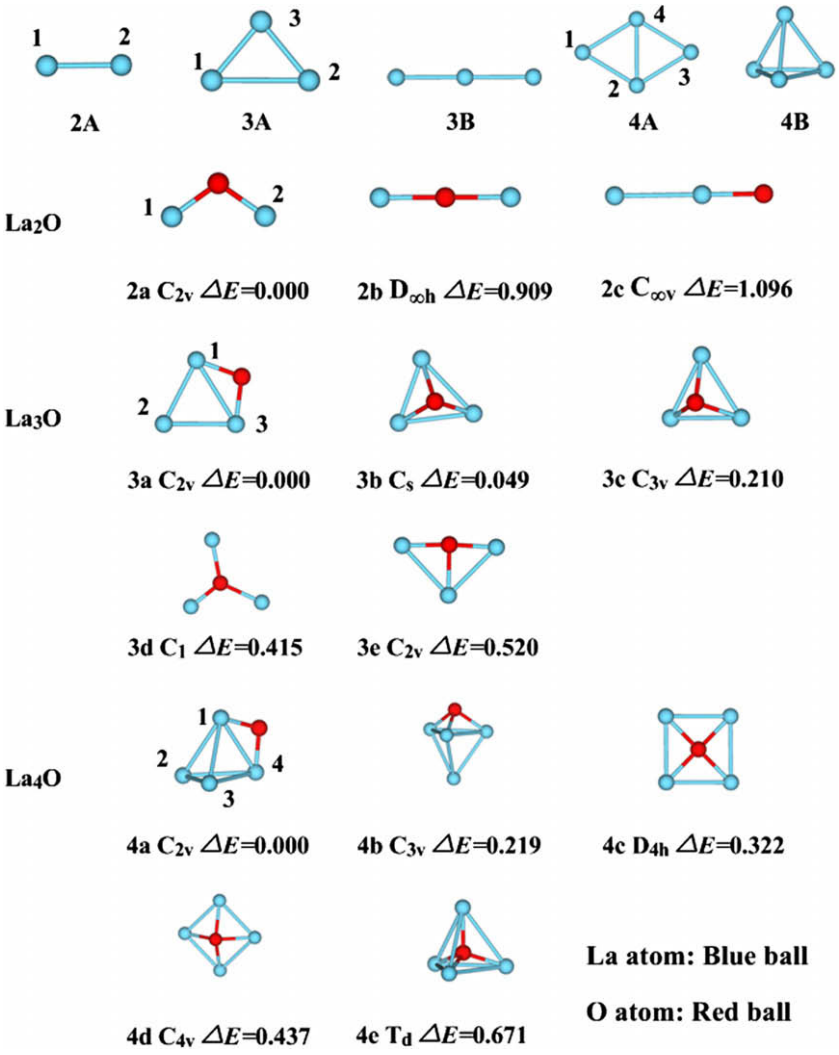

Fig. 1. The stable structures of La_n and La_nO clusters ($2 \leqslant n \leqslant 4$). The La atoms in the lowest-energy structures are labeled by numbers. ΔE is the difference of total binding energy of an isomer from the most favorable isomer (in eV).

proposed in Refs. [6,9] are carefully examined. On the basis of the optimized La_n geometries, different evolution patterns for determining the different sized La_nO isomers, including O-capped, O-substituted, and O-concaved patterns. In addition, the equilibrium geometries of Sc_nO and Y_nO clusters are also considered as the initial structures for La_nO clusters [16,17]. After initial structures are chosen as described above, the optimal configurations are determined automatically by the self-consistent iterations in the geometrical optimizing process. For the lowest-energy structures and some low-lying isomers, we fully re-optimize their possible electronic configurations of total spins. To confirm the stability of structures of both pure lanthanum and lanthanum oxide clusters, the vibrational frequencies are analyzed. All the structures obtained in this work are stable.

Though BPW exchange-correlation potential and DNP basis sets have been sufficiently proven to be satisfactory for Y_n, Sc_nO, and Y_nO clusters [14,16,17], it would be useful to make another brief test in the present work. In order to compare with the available experimental values and previous theoretical works, we calculate bond length and vibration frequency of La_2 dimer. Our results show that the bond length and vibration frequency of the dimer are 2.782 Å and 180.6 cm^{-1}, respectively, which are in agreement with the values of 3.00 Å and 163 cm^{-1} obtained in Ref. [9]. In addition, the bond length of 2.782 Å is also close to another theoretical result, 2.771 Å [6]. More importantly, our theoretical values fit better with the experimental values of 2.80 Å and 230 cm^{-1} than the above two theoretical works [19], implying that the exchange-correlation potential, basis sets and the specific computational parameters used in the calculation are appropriate and the results are reliable.

In addition, in order to verify some of the lowest-energy structures of La_n clusters, we re-optimized their structures at CCSD(T)/LANL2DZ level. The CCSD(T) calculations are performed with GAUSSIAN03 program package [20].

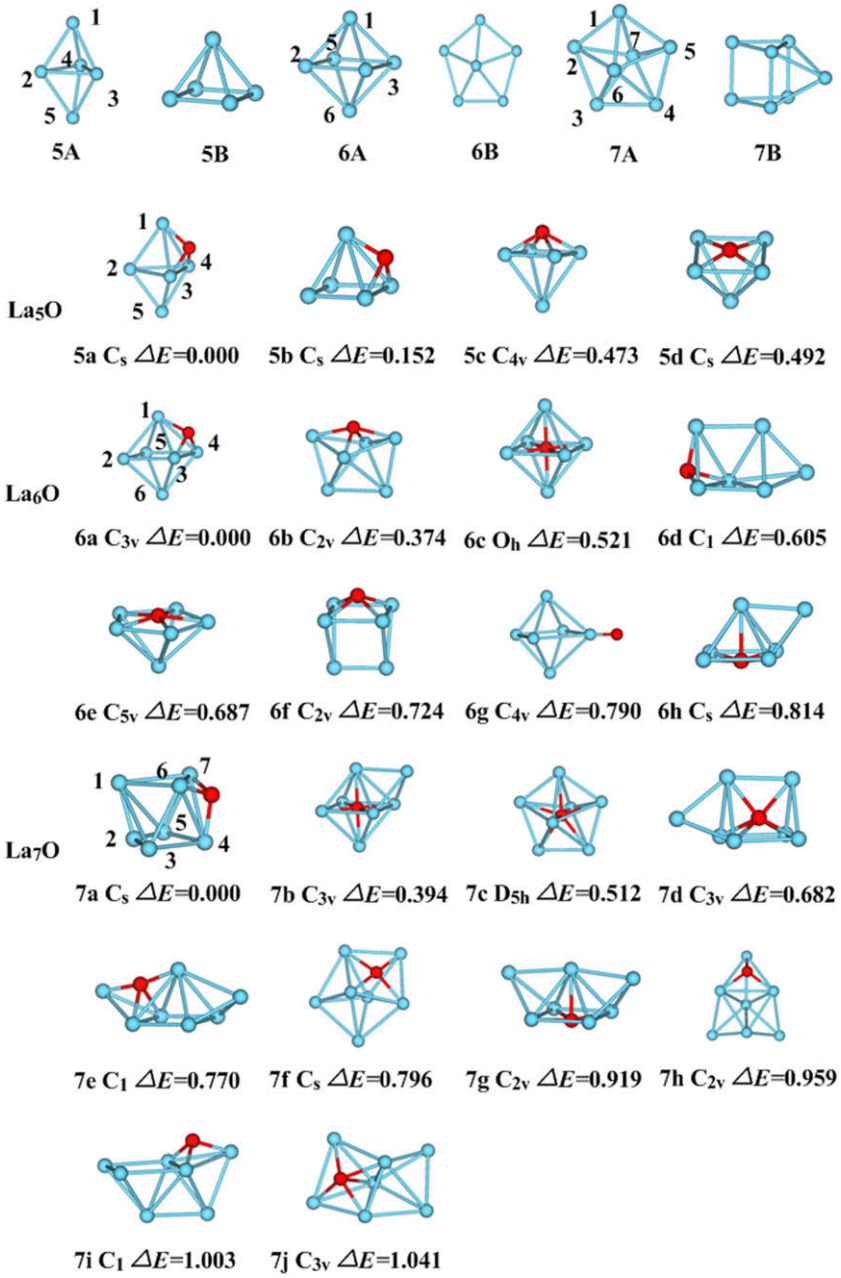

Fig. 2. The same as those in Fig. 1 but for $n = 5–7$.

3. Results and discussion

3.1. The lowest-energy structures of La_n and La_nO clusters

Using the computation scheme described in Section 2, we have explored a number of low-lying isomers and determined the lowest-energy structures. The stable structures of La_n and La_nO clusters are shown in Figs. 1–4. Although we obtained a lot of stable structures for La_n and La_nO clusters at each size, we do not show all of them in the figures for the sake of simplicity. The structures of La_n and La_nO clusters are denoted by number and letter, where the number denotes the La atom number and the letter ranks the isomers in decreasing order of binding-energy. Moreover, theoretical results such as average binding energies, HOMO–LUMO gaps and multiplicities for the lowest-energy structures of the two systems are listed in Table 1.

The dimer La_2 has well established experimental data and has been extensively investigated by different theories. The experimental data and theoretical results about the dimer are summarized in Table 2 [19,6,9,21–24]. It is obvious that our theoretical values, as a whole, are closer to the experimental results on the DFT level. More accurate CCSD(T) method above the DFT level could give more accurate results for the dimer. Though PBEPBE/LANL2DZ method gives a better value of dissociation energy, the bond length is overestimated and the magnetic moment is different from most of the previous DFT results, and is also different from the results of CCSD(T) and CASSCF methods.

For La_3, we optimize six structures, including two linear chains and four triangles. Finally, it is identified that La_3 takes a quartet isosceles triangle (C_{2v}) as its ground state. It has an apex angle of 78.58° and a base side of 3.497 Å. The C_{2v} structure of the trimer is in agreement with previous DFT results [6,9]. In fact, the C_{2v}

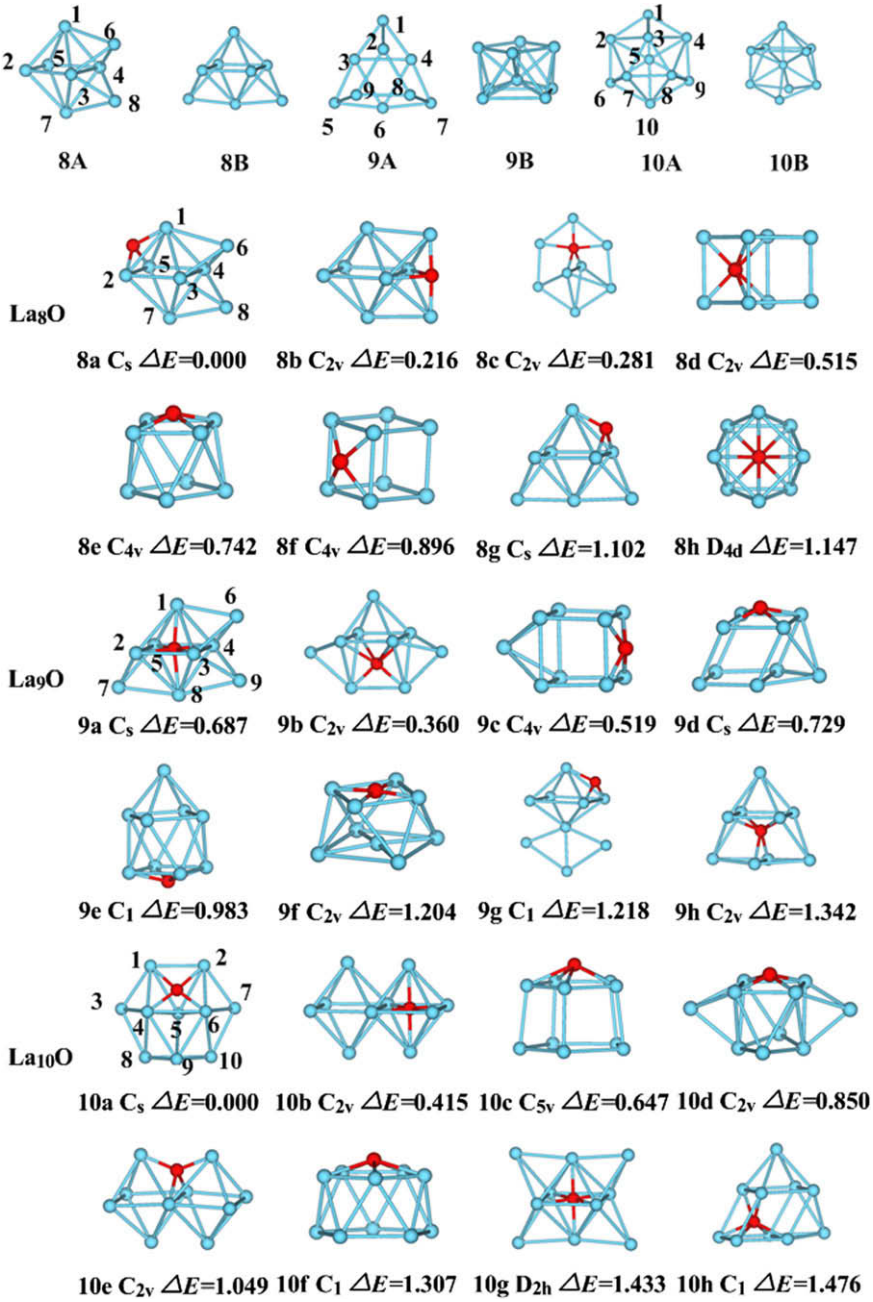

Fig. 3. The same as those in Fig. 1 but for n = 8–10.

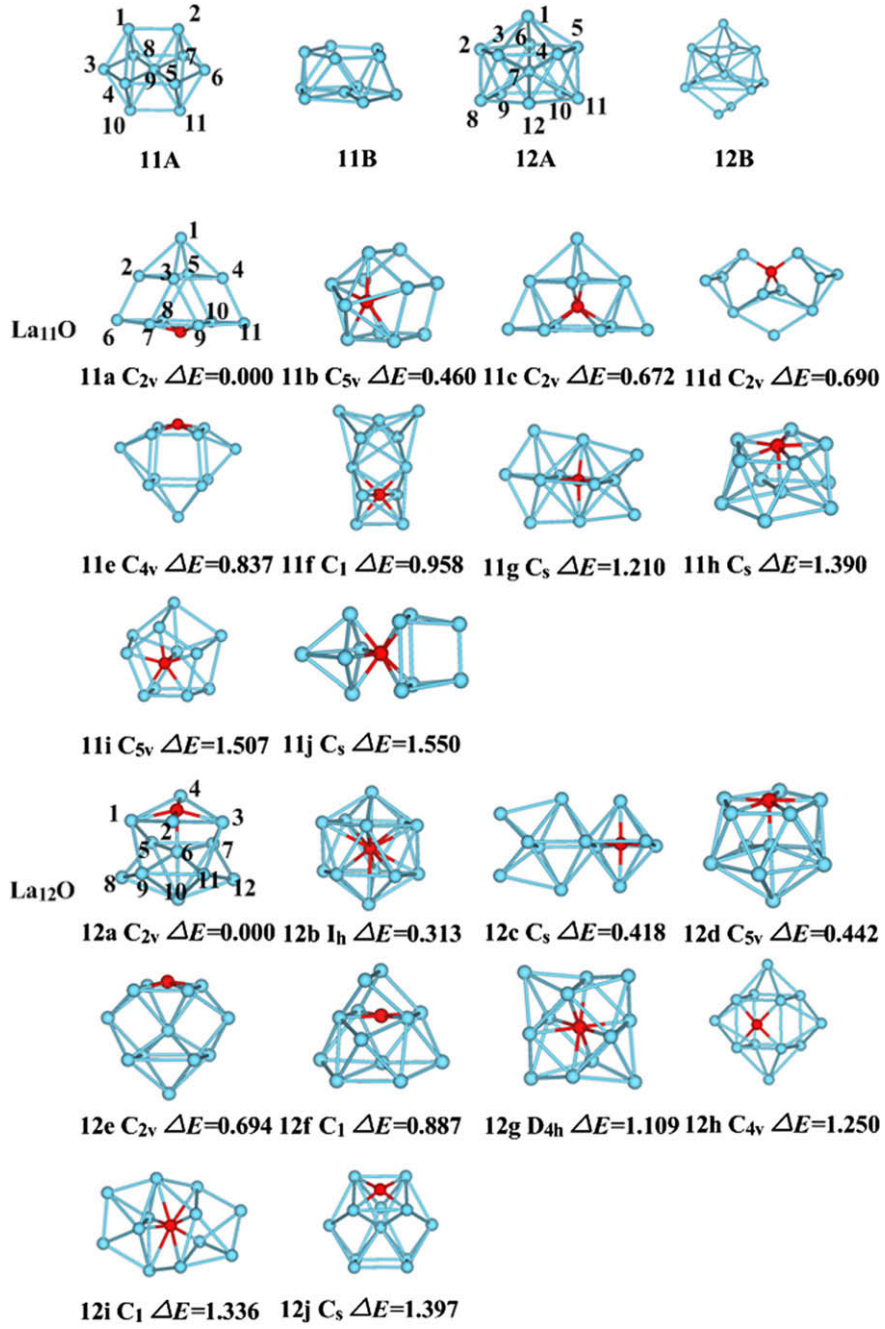

Fig. 4. The same as those in Fig. 1 but for $n = 11$ and 12.

symmetry is also preferred by Y_3 cluster [14]. For La_4, however, previous DFT studies propose different configurations. Zhang and Shen suggest that a C_{3v} structure in a triplet state should be the most stable one while Lyalin et al. find that the lowest-energy structure is a perfect T_d tetrahedron [6,9]. We consider the two structures but find that both of them are the metastable ones at the present computational scheme. The real ground state of La_4 should be a quintet planar rhombus, whose binding energy is far higher than the two structures mentioned above, and this planar rhombus structure has not been discussed previously.

The lowest-energy structures and some metastable structures of $La_{2-4}O$ clusters are also shown in Fig. 1. It is very interesting that the ground states of these smaller clusters prefer to adopt edge-capped configurations, in which the O atom still keeps its two single bonds. For La_2O, similar to Sc_2O and Y_2O, the lowest-energy structure is an isosceles triangle with C_{2v} symmetry [16,17]. The magnetic moment of La_2O is 2 μ_B (see Table 1), which is larger than that of La_2 dimer, 0 μ_B. The lowest-energy structure of La_3O is a distorted planar rhombus, while the lowest-energy structure of La_4O is an edge-capped tetrahedron, which is the first 3D configuration among La_nO clusters. In addition, from Table 1 one can see that the magnetic moments of La_3O and La_4O are smaller than those of the corresponding pure clusters, La_3 and La_4.

A number of initial configurations are considered to obtain the ground states of La_{5-7} clusters. Our results show that the lowest-energy structure of La_5 is a trigonal bipyramid, which is the first 3D configuration among the La_n clusters, as shown in Fig. 2. For La_6 and La_7, it is found that the former has a structure of slightly flattened octahedron, while the latter has a structure of pentagonal bipyramid. Although these lowest-energy configurations (La_{5-7})

Table 1
The spin multiplicity (S), symmetry, binding energy per atom (E_b), HOMO–LUMO gap (E_g), and total magnetic moment (μ_t) for the lowest-energy structures of La_n and La_nO (n = 2–12) clusters.

Cluster	S	Symmetry	E_b (eV)	E_g (eV)	μ_t (μ_B)
La_2	1	$D_{\infty h}$	1.38120	0.962	0
La_3	4	C_{2v}	2.17290	0.344	3
La_4	5	D_{2h}	2.35845	0.193	4
La_5	2	D_{3h}	2.61595	0.410	1
La_6	7	D_{4h}	2.74594	0.281	6
La_7	4	D_{5h}	3.14474	0.518	3
La_8	3	C_{2v}	3.13835	0.276	2
La_9	4	C_{3v}	3.14179	0.278	3
La_{10}	3	C_{3v}	3.31108	0.384	2
La_{11}	2	C_1	3.30340	0.217	1
La_{12}	3	C_{5v}	3.20765	0.112	2
La_2O	3	C_{2v}	4.03070	0.288	2
La_3O	2	C_{2v}	3.91072	0.317	1
La_4O	1	C_{2v}	3.87153	0.354	0
La_5O	2	C_s	3.82523	0.471	1
La_6O	1	C_{3v}	3.64274	0.480	0
La_7O	2	C_s	3.80312	0.296	1
La_8O	3	C_s	3.61953	0.257	2
La_9O	2	C_s	3.76520	0.155	1
$La_{10}O$	1	C_s	3.67161	0.310	0
$La_{11}O$	2	C_{2v}	3.69251	0.064	1
$La_{12}O$	1	C_{2v}	3.87262	0.108	0

Table 2
The magnetic moment μ (μ_B), bond length d (Å), vibrational frequency ω (cm^{-1}), and dissociation energy D_e (eV) of the La_2 dimer.

Method	μ	d	ω	D_e	Reference
BPW/DNP	0	2.78	180.6	2.76	This work
BLYP/DNP	0	2.77		3.08	[6]
PBEPBE/LANL2DZ	1	3.00	163	2.44	[9]
BP86/LANL2DZ	0	2.93	139	1.09	[21]
B3LYP/LANL2DZ	0	2.91	150	1.70	[21]
B3PW91/LANL2DZ	0	2.89	131	1.83	[21]
PBE1PBE/LANL2DZ	0	2.87	136	1.87	[21]
BHLYP/LANL2DZ	0	2.87	161	3.66	[21]
CASSCF	0	2.70	186	2.31	[22]
CCSD(T)	0	2.64	218	2.37	[23]
CISD/SCC	2	3.25	130	1.17	[24]
Experiment		2.80	230	2.5 ± 0.2	[19]

are in good agreement with previous results, the magnetic moment of La_6 is different [6,9]. Refs. [6,9] suggest that the magnetic moment of La_6 cluster is 0 μ_B and 4 μ_B, respectively. Both of the results are different from the value of 6 μ_B obtained in the present work. As mentioned above, experiment data for the moment is 4.8 ± 0.2 μ_B. Therefore, both the values of 4 μ_B and 6 μ_B are reasonable, and we cannot distinguish the true spin multiplicity of the ground state La_6 cluster by the experimental results. More accurate theoretical method may be needed. Here, we employ CCSD(T) method and LANL2DZ basis sets to further investigate the La_6 cluster [20]. In order to avoid excessive calculation, we only performed CCSD(T) calculation on the quintet La_6 and septet La_6. We find that the quintet La_6 is unstable at CCSD(T) level, indicating that the true ground state of La_6 should be septet other than quintet, in consistence with present DFT results. In fact, the CCSD(T) method also supports our conclusion about La_4 cluster, of which the ground state is a planar rhombus with D_{2h} symmetry.

For $La_{5-7}O$ clusters, a notable feature is that the O impurity still prefers to stay outside the clusters, but bonds with three La atoms, forming surface-capped configurations. The lowest-energy structures of La_5O and La_6O can be obtained by directly adding one O atom to the corresponding pure clusters, respectively. For La_7O, the capped pentagonal bipyramid is only a low-lying isomer (see Fig. 2, 7f), whose total energy is higher than that of the ground state 7a (ΔE = 0.796 eV). In addition, we find that the total magnetic moments of La_6O and La_7O are smaller than those of La_6 and La_7, respectively. La_5O has the same magnetic moment as that of La_5, 1 μ_B.

Fig. 3 shows the stable structures of La_{8-10} clusters and $La_{8-10}O$ clusters. Among different isomers of La_8, the C_{2v} bicapped octahedron in a spin triplet state is the lowest-energy configuration. With the same structure, the spin singlet, quintet, and septet states are 0.02, 0.01, and 0.07 eV/atom above the triplet state, respectively (those isomers with the same structure but different spin multiplicities are not given in the figure). The C_{2v} configuration is also adopted by Sc_8 cluster [15]. Our results for La_8 cluster are different from previous conclusions. Lyalin et al. found that a capped pentagonal bipyramid in a singlet state with C_s symmetry should be the most stable one [9]. However, they predicted the magnetic moment of the La_8 cluster is 0 μ_B, which is inconsistent with the experimental data [8]. Another paper suggests that a D_{2d} structure in a triplet state should be the ground state [6]. Again, we perform CCSD(T) calculation on the singlet C_s structure and the triplet D_{2d} structure, respectively. It is very interesting that the initial configuration with D_{2d} symmetry is finally converged to the C_{2v} structure at CCSD(T) level, and the frequency analysis also confirms the stability of the C_{2v} structure. Therefore, we conclude that the real ground state of La_8 should be a C_{2v} structure in a triplet state other than C_s structure or D_{2d} structure.

Similar to La_8, a new lowest-energy structure for La_9 is found. It is a spin quartet state and has a C_{3v} symmetry, which is different from the C_1 symmetry or the D_{3h} symmetry proposed previously [9,6]. We re-optimize these three configurations at CCSD(T) level and find that, indeed, the C_{3v} structure is the most stable. In addition, we could not reproduce the C_1 structure predicted in Ref. [9] under CCSD(T) method. It is noteworthy that though our C_{3v} configuration is in agreement with the more accurate CCSD(T) method, the spin multiplicity is different. The CCSD(T) results suggest that though the quartet state and doublet state are both stable, the sextet state is more favorable. For La_{10}, the bilayer C_{3v} configuration is identified as the lowest-energy structure, which is consistent with the conclusion in Ref. [6]. Interestingly, another tri-layer C_{3v} structure is obtained as the ground state in Ref. [9]. Further investigation shows that this tri-layer structure has an imaginary frequency under present method or CCSD(T) level, though the two imaginary frequencies are different, depending on the details of calculation and method.

From La_8O to $La_{10}O$, several lowest-energy isomers of each cluster size are depicted in Fig. 3. For the ground state structure of La_8O cluster, O atom still prefers to occupy the outer site of the cluster and bonds with three La atoms. It is a spin triplet state and has a C_s symmetry. A similar structure with C_{2v} symmetry is found and identified as the second lowest-energy structure (Fig. 3, 8b). Obviously, the structures of 8a and 8b can be obtained by adding O atom at the different sites of the pure La_8 cluster. For La_9O cluster, however, It is found that the O atom is inserted to the center of the cluster and encapsulated by La atoms. We also consider a lot of isomers in which the O atom is at the outside of cluster, such as 9c–9g, but all of them have higher energies than the ground state 9a. In the case of $La_{10}O$ cluster, the ground state of the cluster is an O-capped C_s structure, and the O atom in the cluster bonds with four surfaced La atoms. A distorted twin octahedron (10b) and a capped pentagonal prism (10c) are found to be the second and the third lowest-energy structures, respectively, as shown in Fig. 3.

Similar to other La_nO clusters (except n = 9), $La_{11}O$ and $La_{12}O$ still tend to adopt the O-capped configurations as their ground states (see Fig. 4, 11a and 12a). The coordinate numbers of O atoms in the two clusters are 4 and 5, respectively. For example, the O atom in $La_{12}O$ cluster bonds with not only four surfaced La atom

but also one central La atom. Generally speaking, the O-capped configuration are universal for the lowest-energy structures of La_nO clusters in the investigated range, and more stable than other isomers. Another interesting aspect is that the coordinate number of O atom in the cluster gradually increases with cluster size. As discussed above, the coordinate numbers of O atom are 2, 3, 4, and 5 for $La_{2-4}O$, $La_{5-8}O$, $La_{10-11}O$ and $La_{12}O$, respectively. This kind of interesting growth pattern is very different from those of Sc_nO and Y_nO clusters [16,17].

The lowest-energy structures of La_{11} and La_{12} clusters are also presented in Fig. 4. The results show that the ground state of La_{11} is a distorted C_1 configuration, which is in agreement with the result in Ref. [9] but different from that in Ref. [6]. On the contrary, our lowest-energy structure for La_{12} is the same as the configuration predicted in Ref. [6] but different from the result of Ref. [9]. Here we do not further perform CCSD(T) calculation on these two largest clusters. In addition, the total magnetic moments of La_{8-12} and $La_{8-12}O$ are listed in Table 1. La_8O has the same total magnetic moments as that of La_8, while the total magnetic moments of $La_{9-12}O$ are smaller than those of the corresponding pure La_n clusters. As a general trend we do not find enhanced magnetic moments in La_nO clusters for $n = 2$–12. In other words, the magnetic behavior of La_nO clusters is different from that of Sc_nO clusters but similar to that of Y_nO clusters [16,17].

We now discuss the relative stability of La_n and La_nO clusters. The relative stability of differently sized clusters can be predicted by calculating the average binding energy and the second-order differences of total energies $E(n)$ defined as $\Delta_2E(n) = E(n+1) + E(n-1) - 2E(n)$. The average binding energies E_b and the second-order differences of total energies $\Delta_2E(n)$ for La_n and La_nO clusters are shown in Fig. 5.

For small pure La clusters the average binding energy increases steadily with the cluster size. The local maxima are found at $n = 7$ and 10 correspond to the most stable structures of the magic La clusters. From the variations of the $\Delta_2E(n)$, one can clearly see that the La_7 and La_{10} clusters are more stable than their neighboring sizes. The higher stability of $n = 7$ is often observed in transition metal clusters including Fe, Ti, Zr, Nb, Pd, and Ta, and can be explained by geometrical close packing with icosahedral growth [25,26]. In comparison with the other group-III elemental clusters, previous DFT studies also indicated that 7-atom cluster are more stable than their neighboring sizes [15,14]. Furthermore, the $\Delta_2E(n)$ curve of La clusters makes a hint about relative stability of the La_3 and La_5 clusters, in addition to the magic clusters La_7 and La_{10}. In fact, for small La clusters ($n \leqslant 7$), odd n gives high stability while even n gives low stability. Around $n = 8$, this behavior is inverted. From $n \geqslant 9$, even n gives more stable clusters than odd n. This indicates that $n = 8$ should be the turning point for the stability of La clusters.

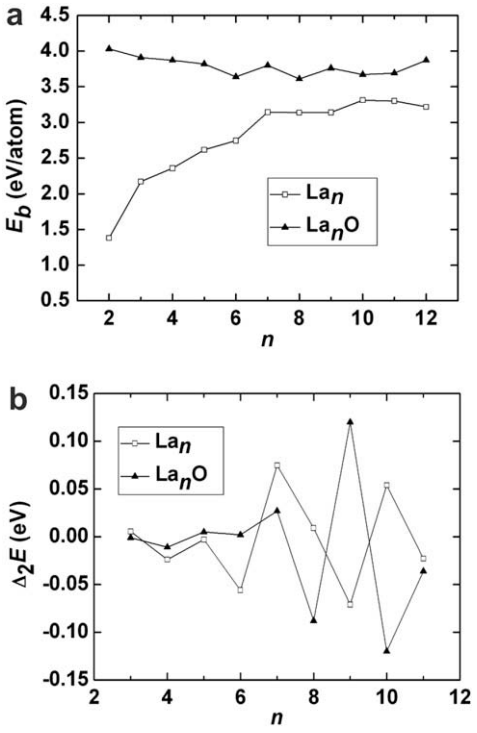

Fig. 5. (a) Size dependence of the binding energy per atom for La_n and La_nO clusters. (b) Second-order differences of total energy for La_n and La_nO clusters.

For La_nO clusters, however, the bonding energy curve gradually decreases at $n \leqslant 6$ but slowly increases at $n \geqslant 10$, and forms two small peaks at $n = 7$ and 9, implying that La_7O and La_9O clusters are more stable. The curve does not exhibit evident quantum size effects or big jumps. Similar trends are also found in Y_nO and Sc_nO clusters, though the local minima or maxima of the curves are different, depending on the specific systems [16,17]. Moreover, the average binding energies of La_nO are far higher than those of La_n clusters at smaller sizes, and the binding-energy differences of the two systems gradually decrease with the cluster size. Generally speaking, the doping of O atom can greatly improve the stability of La clusters with smaller sizes.

3.2. Electronic properties

The ionization potential (IP) and the electron affinity (EA) are two important quantities which can provide fundamental tools to insight into the size-dependent evolution of electronic properties and to distinguish isomers that possess different energies. Although previous DFT studies have presented the stable structures, HOMO–LUMO gaps and magnetic moments of La_n clusters, the IPs and EAs of clusters are still unknown [6,9]. In this paper, we systematically and carefully calculated the vertical IPs and vertical EAs of La_n and La_nO clusters. The vertical IP is calculated from $IP = E_n - E_n^+$, where E_n^+ is the total energy of the cationic cluster at the corresponding neutral geometry, while the vertical EA is calculated from $EA = E_n - E_n^-$, where E_n^- is the total energy of anionic cluster at the corresponding neutral geometry.

The vertical IPs and vertical EAs are shown in Fig. 6. Generally speaking, the IPs and EAs of La_nO clusters exhibit a similar trend as the pure clusters. For La clusters, the IPs gradually decrease with cluster size for $n \leqslant 6$ but show an oscillatory behavior for $n \geqslant 7$. The dimer La_2 has the highest IP value, 4.332 eV, while La_6 has the lowest one, 2.961 eV. Two significant peaks are found at $n = 7$ and 10, which further confirm the high stability of La_7 and La_{10} clusters. Furthermore, the local peak in EA curve at $n = 5$, 7, and 10 also hints the stability of 5-atom, 7-atom, and 10-atom clusters. These results agree with above analysis from E_b and $\Delta_2E(n)$.

For La_nO clusters, however, the local peaks are found at 3, 7, and 10 for IPs and 6, 9, and 11 for EAs. It seems that there is not a strong correlation between the stability of the clusters and the IPs or EAs. The IPs gradually decrease with the cluster size while the EAs has an opposite trend. The EA values of La_nO clusters are usually smaller than those of La clusters except $n = 9$. It is mentioned that there is a sharp increase from $n = 8$ to 9 for the EA curve of La–O clusters, which induces a larger EA value of cluster La_9O.

Usually, the energy gap between HOMO and LUMO is considered to be a good indicator of the electronic stability for small clusters. Table 1 presents the energy gaps of the lowest-energy isomers for La_n and La_nO clusters. For pure lanthanum clusters, the highly stable species, such as La_5, La_7, and La_{10}, indeed have a larger gaps, and the local minima for La_4 and La_6 are consistent with the less

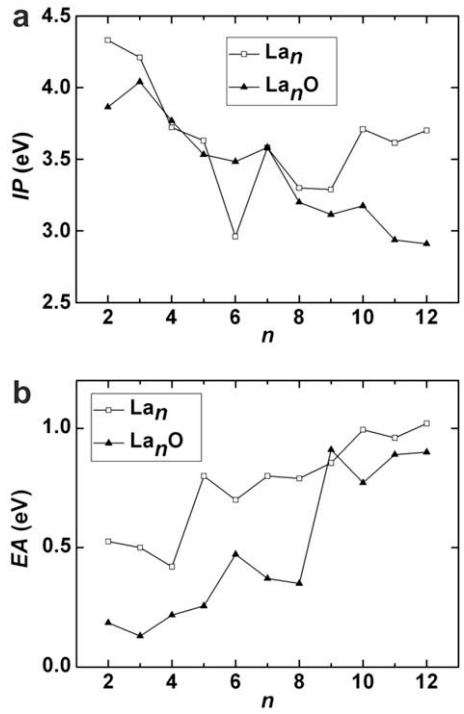

Fig. 6. (a) Vertical IPs of La_n and La_nO clusters. (b) Vertical EAs of La_n and La_nO clusters.

stable sizes found in second-order energy difference. However, for La_nO, it is obvious that the HOMO–LUMO gaps listed in Table 1 could not well reflect the stability of clusters. For example, the highly stable cluster La_9O only has a very small gap value, 0.155 eV. In a word, the IPs, EAs, and gaps can well describe the stability of the pure lanthanum clusters, but this significant rule is destroyed after doping O atom.

We performed Mulliken population analysis for the ground state structures and the atomic charges of O atom of the clusters La_nO are plotted in Fig. 7. The charges on O atom, ranging from ~ -0.8 e to -0.95 e, clearly indicate that there is an obvious electron transfer from La atoms to O atom and that the La atoms and O atom heavily interact. It should be a very important reason for the enhanced stability of La_nO clusters.

3.3. Local magnetic moment and magnetic ordering

As mentioned in Section 1, detailed data on the magnetic behavior of lanthanum clusters in the size range of 5–20 atoms have become available from molecular beam deflection experiment very recently [8]. In Fig. 8, our theoretical results are compared well with the experimental values. The size dependence of the theoretical results is generally consistent with the experimental trend. The agreement implies that the accurate first-principle determination is appropriate and our theoretical results could verify the experimental observation.

The experiment measured only the total magnetic moments of clusters, and there is no direct indication of the nature of the magnetic ordering displayed in these clusters. Actually, the magnetic behavior can be ferromagnetic (FM), where spins are aligned in parallel directions, or antiferromagnetic (AFM), where some spins are antiparallel to other ones. Here, we systematically investigate the local moments of clusters and the detailed data are listed in Table 3. For La clusters, both the FM and AFM are found in the investigated range. The spins on La atoms are all parallel for the clusters with $n \leqslant 4$. The first appearance of AFM coupling takes place at $n = 5$, in which the La 1 and La 5 atoms align antiparallel to those the remaining three atoms. Similar to La_5, La_7, and La_{12} clusters also prefer to adopt AFM ordering. For other sizes, the magnetic orderings of the clusters are all FM. The trend of FM-to-AFM transition in La clusters is quite different from those in Sc and Y clusters [14,15].

In La_nO clusters, the impurity O atom always exhibits a small negative local moment, as shown in Table 3. We find that the local moment of O atom is antiferromagnetically coupled to those of the surrounding La atoms for smaller clusters ($n = 2$ and 3). For some larger clusters, such as La_4O, La_6O, $La_{10}O$, and $La_{12}O$, the total magnetic moments are quenched due to the closed-shell electronic configuration, and the results further show that the local moment on each atom of these clusters is zero. In addition, in $La_{11}O$ cluster, the O moment is ferromagnetically coupled to the surrounding La 7, La 8, La 9, and La 10 atoms. For other clusters, the O atom is simultaneously ferromagnetically or antiferromagnetically coupled to the surrounding La atoms. In a word, the magnetic ordering of La_nO clusters is more complicated than the pure La_n clusters.

Finally, we will explore the nature of bonding in pure La_n clusters. Previous study only points out that the small La clusters are nonmetallic and that the convergence to the metallic bulk phase is slow [6]. Therefore further investigation is necessary. In order to gain more information about the bonding characteristics of La_n clusters, Mulliken population analysis and Mayer bond order calculations are performed.

The calculations of Mayer bond orders reveal that the average bond order between the nearest-neighbor La atoms decreases from 2.971 for La_2 to 0.792 for La_7, and gradually reaches to 0.556 for La_{12}. This indicates that the bonding in La clusters has the covalence character and that the covalence bonds are slowly weakened with the increase of cluster size. In addition, there is no clear hint for a transition from nonmetallic to metallic systems in our studied sizes.

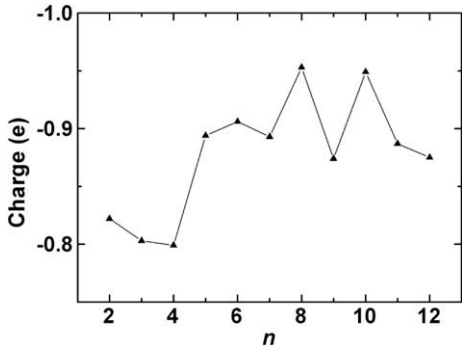

Fig. 7. Atomic charges of O atom of La_nO clusters for the lowest-energy structures.

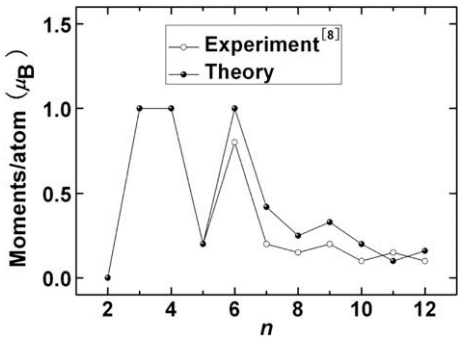

Fig. 8. The magnetic moments (μ_B/atom) of La_n clusters.

Table 3
The local magnetic moments for the lowest-energy structures of La_n and La_nO (n = 2–12) clusters. μ_i is the local moment of the ith La atom and μ_O is the local moment of the O atom.

Cluster	Local magnetic moment (μ_B)
La_2	$\mu_{1,2} = 0$
La_3	$\mu_{1,2} = 0.861$, $\mu_3 = 1.279$
La_4	$\mu_{1,3} = 1.473$, $\mu_{2,4} = 0.527$
La_5	$\mu_{1,5} = 0.929$, $\mu_{2-4} = -0.286$
La_6	$\mu_{1,6} = 1.193$, $\mu_{2-5} = 0.904$
La_7	$\mu_{1-5} = 0.676$, $\mu_{6,7} = -0.189$
La_8	$\mu_{1,7} = 0{,}522$, $\mu_{2,5} = -0.072$, $\mu_{3,4} = 0{,}218$, $\mu_{6,8} = 0.331$
La_9	$\mu_{1,5,7} = 0.222$, $\mu_{2,8,9} = 0.501$, $\mu_{3,4,6} = 0.277$
La_{10}	$\mu_{1,6,9} = 0.221$, $\mu_{2,4,10} = 0.205$, $\mu_{3,7,8} = 0.209$, $\mu_5 = 0.098$
La_{11}	$\mu_{1,4,8,10} = 0.123$, $\mu_{2,5,7,11} = 0.125$, $\mu_{3,6} = 0.004$, $\mu_9 = 0.001$
La_{12}	$\mu_1 = -0.696$, $\mu_7 = -0.046$, $\mu_{2-6,8-12} = 0.425$
La_2O	$\mu_O = -0.023$, $\mu_{1,2} = 1.011$
La_3O	$\mu_O = -0.008$, $\mu_{1,3} = 0.263$, $\mu_2 = 0.482$
La_4O	$\mu_O = 0$, $\mu_{1-4} = 0$
La_5O	$\mu_O = -0.014$, $\mu_1 = 0.420$, $\mu_2 = 0.414$, $\mu_{3,4} = -0.008$, $\mu_5 = 0.196$
La_6O	$\mu_O = 0$, $\mu_{1-6} = 0$
La_7O	$\mu_O = -0.003$, $\mu_1 = 0.157$, $\mu_2 = 0.201$, $\mu_{3,5} = 0.188$, $\mu_4 = 0.062$, $\mu_{6,7} = 0.104$
La_8O	$\mu_O = -0.001$, $\mu_1 = -0.085$, $\mu_{2,5} = 0.052$, $\mu_{3,4} = 0.079$, $\mu_6 = 0.507$, $\mu_7 = 0.501$, $\mu_8 = 0.814$
La_9O	$\mu_O = -0.005$, $\mu_1 = 0.106$, $\mu_{2,5} = 0.320$, $\mu_{3,4} = -0.037$, $\mu_6 = 0.009$, $\mu_7 = 0.599$, $\mu_8 = 0.110$, $\mu_9 = -0.386$
$La_{10}O$	$\mu_O = 0$, $\mu_{1-10} = 0$
$La_{11}O$	$\mu_O = -0.011$, $\mu_1 = -0.042$, $\mu_{2,4} = 0.337$, $\mu_{3,5} = 0.196$, $\mu_{6,11} = 0.073$, $\mu_{7-10} = -0.040$
$La_{12}O$	$\mu_O = 0$, $\mu_{1-12} = 0$

In order to illustrate the existence of the ionic character in La clusters, we carried out Mulliken population analysis for each atomic site. As a representative, the Mulliken charge for each atomic site and deformation electron density computed from the total electron density with the density of the isolated atoms subtracted for the ground state structures of the La_7 and La_{10} clusters are shown in Fig. 9a and b, respectively. Qualitatively, the ionic bonding can be identified by the charge transfer from cation to anion. Taking La_7 as an example, from Fig. 9a it is obvious that there is a net electron transfer from La 1, La 2, La 3, La 4, and La 5 atoms to La 6 and La 7 atoms, clearly indicating that the La–La bonding in small La clusters has the ionic character. Moreover, the electron deformation density (see Fig. 9b) distributes not only around the La atoms but also in the intervals of cluster, further verifying that the co-existence of ionic and covalent bonding characteristics in small La clusters, which is in consistent with above analysis. As the cluster size further increases, the pure La clusters should have certain character of metallic bonding, and the bonding of larger La clusters may simultaneously have the covalent, ionic, and metallic characteristics.

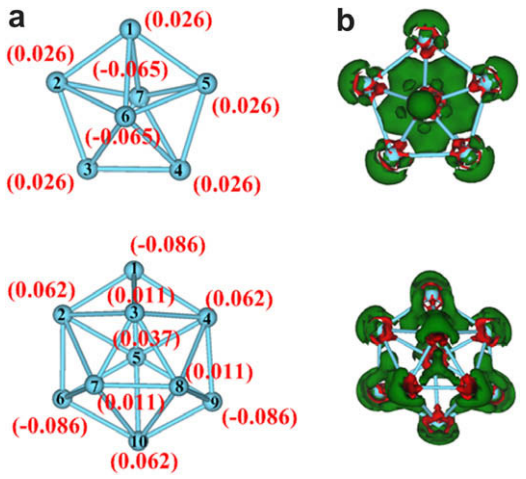

Fig. 9. (a) On-site Mulliken charge distribution (numbers in parentheses) and (b) deformation electron density of La_7 and La_{10} clusters.

4. Conclusions

The equilibrium geometries, stabilities, electronic properties, and magnetic properties of different-sized La_n and La_nO (n = 2–12) clusters are investigated in the present paper. All the results are summarized as follows:

(1) For pure La clusters, the structures of La_4, La_8, and La_9 are the new ones that have not been proposed in previous literature. These structures are more stable, as confirmed by more accurate CCSD(T) method. For La_nO clusters, we find that the O atom prefers to stay outside the cluster, and the coordination number of O atom gradually increases with cluster size. This kind of growth pattern is different from those of Sc_nO and Y_nO clusters.
(2) According to the calculated average binding energies and $\Delta_2E(n)$, the relative stabilities of La_n clusters are gradually strengthened with increase of the size, and the La_3, La_5, La_7, and La_{10} are more stable than others. Furthermore, the doping of O atom can greatly improve the stability of small La_n, and the enhanced stability should attribute to the heavy interaction between O atom and La atoms.
(3) The vertical IPs, vertical EAs, and HOMO–LUMO gaps of La_n and La_nO clusters are systemically investigated and discussed. Generally speaking, the three quantities could well reflect the stability of La_n clusters. However, we do not find a strong correlation between the stability and the three physical quantities for La_nO clusters, implying that the O atom could greatly change the electronic properties of La_n clusters.
(4) The total magnetic moments, the local magnetic moments and the average magnetic moments are carefully investigated. The total magnetic moments of La_nO clusters are, as a whole, smaller than or equal to the corresponding La_n clusters and quenched at n = 4, 6, 10, and 12. The magnetic behavior of La_nO clusters is different from that of Sc_nO clusters, in which enhanced magnetic moments are found. In addition, we find that all the La_n clusters except La_5, La_7, and La_{12} have FM ordering. The trend of FM-to-AFM transition in pure La clusters is different from that of Sc and Y clusters. The magnetic ordering of La_nO are more complicated. Furthermore, our calculated average magnetic moments of La_n are in good agreement with the experimental data, indicating that the present treatments are reliable and reasonable.
(5) The analysis of the nature of bonding in small La_n indicates that small La_n clusters are nonmetallic, which agrees with previous theoretical results. Here, we further point out that the ionic and covalent bonding characteristics are important in small La clusters by discussing the Mulliken population analysis and Mayer bond orders. In addition, we find that there is no clear hint for a transition from nonmetallic to metallic systems for La clusters in our studied sizes.

We hope that the present work could give a better understanding about the group-III transition metal clusters and their oxides.

Acknowledgements

This work was supported by the State Key Programs for Basic Research of China (Grant Nos. 2005CB623605 and 2006CB921803),

and by National Foundation of Natural Science in China Grant Nos. 60676056 and 10874071.

References

[1] G. Seifert, Nat. Mater. 3 (2004) 77.
[2] S.N. Khanna, P. Jena, Phys. Rev. Lett. 69 (1992) 1664.
[3] B.K. Rao, P. Jena, M. Manninen, R.M. Nieminen, Phys. Rev. Lett. 58 (1987) 1188.
[4] Y.H. Luo, Y.Z. Wang, Phys. Rev. A 64 (2001) 015201.
[5] S. Erkoc, T. Bastug, M. Hirata, S. Tachimori, Chem. Phys. Lett. 314 (1999) 203.
[6] D.B. Zhang, J. Shen, J. Chem. Phys. 120 (2004) 5104.
[7] D.B. Zhang, J. Shen, J. Chem. Phys. 120 (2004) 5081.
[8] M.B. Knickelbein, Phys. Rev. B 71 (2005) 184442.
[9] A. Lyalin, A.V. Solov'yov, W. Greiner, Phys. Rev. A 74 (2006) 043201.
[10] N. Liu, Q.M. Ma, Z. Xie, Y. Liu, Y.C. Li, Chem. Phys. Lett. 436 (2007) 184.
[11] D.B. Zhang, J. Shen, J. Chem. Phys. 123 (2005) 154313.
[12] D.B. Zhang, J. Shen, J. Chem. Phys. 120 (2005) 114305.
[13] Z.D. Reed, M.A. Duncan, J. Phys. Chem. A 112 (2008) 5354.
[14] H.K. Yuan, H. Chen, A.L. Kuang, A.S. Ahmed, Z.H. Xiong, Phys. Rev. B 75 (2007) 174412.
[15] J.L. Wang, Phys. Rev. B 75 (2007) 155422.
[16] Z. Yang, S.J. Xiong, J. Chem. Phys. 129 (2008) 124308.
[17] Z. Yang, A.M. Guo, H.J. Zhu, S.J. Xiong, J. Phys. Chem. A, submitted for publication.
[18] DMOL is a density functional theory program distributed by Accelrys Inc. B. Delley, J. Chem. Phys. 92 (1990) 508;
J.P. Perdew, Y. Wang, Phys. Rev. B 45 (1992) 13244;
D. Becke, Phys. Rev. A 38 (1988) 3098.
[19] G. Verhaegen, S. Smoes, J. Drowart, J. Chem. Phys. 40 (1964) 239.
[20] M.J. Frish, G.W. Trucks, H.B. Schlegel, et al., GAUSSIAN03, E.01, Pittsburgh, PA, 2003.
[21] Z.J. Wu, J.S. Shi, S.Y. Zhang, H.J. Zhang, Phys. Rev. A 69 (2004) 064502.
[22] X. Cao, M. Dolg, Theor. Chem. Acc. 108 (2002) 143.
[23] X. Cao, M. Dolg, Mol. Phys. 101 (2003) 1967.
[24] M. Dolg, H. Stroll, H. Preuss, J. Mol. Struct.: THEOCHEM 277 (1992) 239.
[25] V. Kumar, Y. Kawazoe, Phys. Rev. B 66 (2002) 144413.
[26] M. Sakurai, K. Watanabe, K. Sumiyama, K. Suzuki, J. Chem. Phys. 111 (1999) 235.